Intracellular temperature mapping with fluorescence-assisted photoacoustic thermometry

Liang Gao, Chi Zhang, Chiye Li, Lihong Wang

Liang Gao, Chi Zhang, Chiye Li, Lihong Wang, "Intracellular temperature mapping with fluorescence-assisted photoacoustic thermometry," Proc. SPIE 8943, Photons Plus Ultrasound: Imaging and Sensing 2014, 894309 (3 March 2014); doi: 10.1117/12.2038569

SPIE.

Event: SPIE BiOS, 2014, San Francisco, California, United States

Intracellular temperature mapping with fluorescence-assisted photoacoustic-thermometry

Liang Gao, Chi Zhang, Chiye Li, and Lihong Wang†
Optical Imaging Laboratory, Department of Biomedical Engineering, Washington University in St. Louis., St. Louis, MO 63130, USA
†LHWANG@WUSTL.EDU

ABSTRACT

Measuring intracellular temperature is critical to understanding many cellular functions but still remains challenging. Here we present a technique – fluorescence-assisted photoacoustic thermometry (FAPT) – for intracellular temperature mapping applications. To demonstrate FAPT, we monitored the intracellular temperature distribution of HeLa cells with sub-degree (0.7 ^{o}C) temperature resolution and sub-micron (0.23 μm) spatial resolution at a sampling rate of 1 kHz. Compared to traditional fluorescence-based methods, FAPT features the unique capability of transforming a regular fluorescence probe into a concentration- and excitation-independent temperature sensor, bringing a large collection of commercially available generic fluorescent probes into the realm of intracellular temperature sensing.
Keywords: Photoacoustic microscopy, Temperature imaging

1. INTRODUCTION

Many cell events, such as cell division, nutrient metabolism, and gene expression, are accompanied by intracellular temperature change [1-3]. Accurately measuring this temperature change can, in turn, contribute to a deeper understanding of biochemical processes inside a cell. Although cellular thermometry has been realized at the single-cell level by employing tools such as micro- or nano-scale thermocouples[4, 5], fluorescence nanoparticles or nanogels [6, 7], and a photoacoustic thermometer [8], most of these techniques have treated the cell as a whole and measured its average temperature. Knowledge of the average cellular temperature is, however, insufficient for exploring thermogenesis and thermal dynamics at the level of subcellular structures [2].

Achieving intracellular temperature mapping is difficult because it requires measuring a physical quantity sensitive to local temperature changes but independent of the sensor's concentration and excitation strength. To our knowledge, only two fluorescence-based techniques have realized intracellular temperature mapping, utilizing fluorescence lifetime [9] and polarization anisotropy [10], respectively. Despite the high spatial and temperature resolution they have accomplished in cellular imaging experiments, both methods rely on custom-developed fluorescent biosensors, limiting their accessibility to only a few laboratories.

A major impetus towards the widespread application of fluorescence microscopy is the ongoing development of fluorescent probes, which display excellent selective labeling of cellular structures [11]. However, most commercially available fluorescent probes were not intended to be temperature sensitive. To expand the toolbox of intracellular temperature mapping technique and make it accessible to a much broader biological research community, here we present a novel method – fluorescent-assisted photoacoustic thermometry (FAPT) – which integrates fluorescence microscopy with photoacoustic thermometry on one platform. FAPT features the unique capability of transforming a generic fluorescent probe into a concentration- and excitation-independent intracellular temperature sensor.

2. PRINCIPLE

Upon absorbing a photon, a fluorophore's electron transits from the ground state to an excited state. The electron's energy is released primarily via two paths [12, 13]: radiative decay, *i.e.*, fluorescence, or non-radiative decay, *i.e.*, thermal dissipation. The possibility of an electron following either of these two decay approaches is described by the fluorophore's quantum yield η. After excitation, the emitted fluorescence intensity equals

$$I_f = AF\mu_a\eta, \quad (1)$$

Photons Plus Ultrasound: Imaging and Sensing 2014, edited by Alexander A. Oraevsky, Lihong V. Wang,
Proc. of SPIE Vol. 8943, 894309 · © 2014 SPIE · CCC code: 1605-7422/14/$18 · doi: 10.1117/12.2038569

where A is a constant, F is optical fluence (J/cm^2), and μ_a is the absorption coefficient (cm^{-1}). μ_a is dependent on the fluorophore's concentration and its molecular absorption cross-section.

On the other hand, if the excitation light is a short pulse, the generated heat during non-radiative decay produces an ultrasonic wave via thermoelastic expansion. The detected photoacoustic amplitude is [14]

$$P = BF\mu_a(1-\eta)\Gamma . \tag{2}$$

In Eq. 2, B is a constant, and Γ is the Grueneisen coefficient, which is temperature dependent by an empirical relation [15]

$$\Gamma = C_1 + C_2 T , \tag{3}$$

where T is the local temperature, and C_1 and C_2 are constants.

Traditional photoacoustic thermometry [15-17] calculates the temperature map from Eq. 2 and Eq. 3, *i.e.*,

$$T(x,y) = \frac{1}{C_2 B}\frac{1}{1-\eta}\frac{P(x,y)}{F(x,y)\mu_a(x,y)} - \frac{C_1}{C_2}. \tag{4}$$

However, the temperature mapping derived by Eq. 4 is affected by the F and μ_a distributions – it is accurate only when μ_a can be considered as uniform and F can be accurately measured.

To eliminate the effect of μ_a and F on the temperature mapping measurement, we collect fluorescence and photoacoustic (PA) signals simultaneously at each scanning point. Substituting μ_a in Eq. 4 with the corresponding fluorescence intensity in Eq. 1 gives

$$T(x,y) = \frac{A}{C_2 B}\frac{\eta}{(1-\eta)}\frac{P(x,y)}{I_f(x,y)} - \frac{C_1}{C_2}. \tag{5}$$

In FAPT, a new quantity R is defined as the ratio of the photoacoustic amplitude P to the fluorescence intensity I_f. For a fluorophore whose quantum yield η is insensitive to temperature changes, Eq. 5 can be simplified as

$$T(x,y) = D_1 R(x,y) - D_2 , \tag{6}$$

where $R = P/I_f$, and the coefficients $D_1 = A\eta/C_2B(1-\eta)$ and $D_2 = C_1/C_2$ are independent of μ_a and F and remain constant for the same fluorophore. Because D_1 and D_2 can be calibrated for, the corresponding local temperature can be derived by measuring the ratio R at each scanning point.

The uncertainty of the derived temperature from Eq. 5 can be estimated as

$$\frac{|\Delta T|}{T} \approx \sqrt{(\frac{\Delta P}{P})^2 + (\frac{\Delta I_f}{I_f})^2} . \tag{7}$$

On the one hand, the noise contributed by the fluorescence was considered as shot-noise limited, and calculated as

$$\frac{|\Delta I_f|}{I_f} = \frac{1}{\sqrt{N}} , \tag{8}$$

where N is the number of fluorescent photons that the system acquired. On the other hand, the noise item contributed by PA is normally dominated by thermal noise and interference noise [18], which depend highly upon the specifics of the experimental setup.

3. SYSTEM DESCRIPTION

The FAPT was built on a previously described sub-micron resolution PAM system [19]. The system setup is shown in Fig. 1. A pulsed laser (wavelength: 532 nm, pulse duration: ~5 ns) both excited the fluorescence and generated

photoacoustic signals. Two objectives, with NA=0.32 (Leitz Wetzlar Phaco 10×) and NA=1.40 (Olympus PLAPO 60×), focused the excitation laser and collected the fluorescence signal. The spatial resolutions corresponding to these two objectives were 0.82 μm and 0.23 μm, respectively. A combination of an excitation filter (central wavelength 532 nm, bandwidth 3 nm), a dichroic beamsplitter (transmission wavelength 400-530 nm, reflection wavelength 575 nm-725 nm), and an emission filter (central wavelength 559 nm, bandwidth 34 nm) separated excitation light from fluorescence. The fluorescent light was detected by a photomultiplier tube (PN: PMM01, Thorlabs Inc.), while the PA signal was acquired by a custom-made focused ultrasound transducer with a central frequency of 40 MHz and a numerical aperture of 0.5. In order to obtain a 2D temperature map, the sample was raster scanned across the region of interest.

The sample was immersed in phenol-red free medium (PN: 21063-029, Life technologies) in an incubator chamber (PN: CSC-25, Bioscience Tools), whose temperature could be finely adjusted (step: 0.01°C) by the accompanying controller (PN: TC-1-100s, Bioscience Tools). The temperature of the incubator chamber was monitored by a thermocouple immersed in the bath.

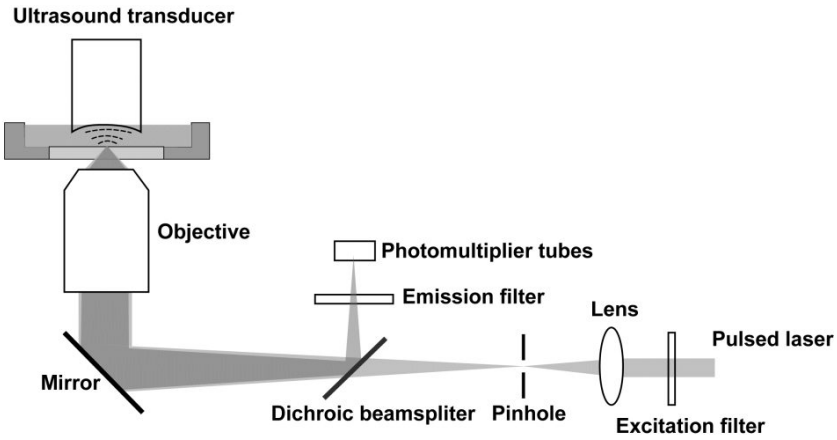

Fig. 1. FAPT system setup. The fluorescence and PA signals were measured simultaneously at each scanning point.

4. RESULTS AND DISCUSSION

We applied FAPT to cellular temperature imaging. A mitochondrion is a cellular organelle that produces energy and heat via oxidization. Temperature imaging of mitochondria would help to understand cellular metabolism [2]. Here we stained HeLa cells (30-40 microns in diameter) with a commercially available fluorescent dye – MitoTracker orange (PN: M-7510, Life technologies, Inc.) and monitored the mitochondria temperature during environmental temperature changes.

The HeLa cells grew in Dulbecco's Modified Eagle Medium with 10% fetal bovine serum and 1% penicillin/streptomycin supplement. The cells were incubated at 37 °C in 5% CO_2 and split every 72 hours. After being dispersed in 0.25% EDTA-trypsin, they were seeded at $2\text{-}4\times10^4$ cells per square centimeter. Culture medium was removed 24 hours after imbedding cells on a cover glass and replaced by staining solution, a fresh culture medium containing 10 μM MitoTracker Orange probes (PN: M-5710, Life technologies). After incubation in staining solution for 60 minutes, the cells were rinsed twice with fresh medium. After staining, cells were trypsinized, collected and suspended in extraction buffer (PN: FNN0011, Life technologies). To inhibit proteolysis, 50 μL of protease inhibitor cocktail (PN: P2714, Sigma-Aldrich) for each milliliter of buffer and 0.5 mM phenylmethanesulfonyl fluoride (PN: P7626, Sigma-Aldrich) were added before the extraction. The cells with the extraction solution ware kept on ice for 40 minutes with occasional vortexing. The lysate was clarified by centrifugation at 13000×g for 15 mins.

To be eligible for FAPT imaging, the quantum yield of the chosen fluorescent dye must be temperature-insensitive. Since insensitivity had not been reported for the fluorescent dye MitoTracker orange, we first measured it in an aqueous solution. By exciting the fluorophore and collecting the corresponding fluorescence at each temperature, the relation between fluorescence intensity and temperature was acquired (Fig. 2a). The result shows that the quantum yield of MitoTracker orange is stable over 25 °C – 37 °C, a temperature range of interest in cellular studies [9, 10].

Then, we calibrated the relation between the PA/fluorescence ratio *R* and temperature for MitoTracker orange in cell extract (Fig. 2b). The coefficient of determination is 0.995 for the linear fit. The SNR of the measured PA and fluorescence signals were 33 dB and 49 dB, respectively, resulting in ~0.7 °C temperature resolution in this experiment.

Next, the HeLa cells stained with MitoTracker orange were imaged by FAPT at environmental temperatures of 36.0 °C and 27.0 °C. The microscope objective (Olympus PLAPO 60×) with NA=1.4 focused excitation light and collected fluorescence. Figs. 2(c)-(e) show the measured PA, fluorescence, and FAPT-recovered mitochondrial temperature map acquired at 36 °C, respectively. Figs. 2(f)-(h) show the corresponding images acquired at 27 °C. Since MitoTracker orange was selectively stained on the mitochondria, few photoacoustic and fluorescence signals were measured in other cellular organelles. The unknown temperature outside mitochondria was pseudo-colored as dark blue in Figs. 2e and 2h. The mean values of recovered cellular temperature in Fig 2e and 2h are 35.9 °C and 27.0 °C, respectively, in good agreement with the corresponding environmental temperatures.

5. CONCLUSION

In summary, we presented a generic technique, FAPT, for intracellular temperature mapping applications. Cellular experiments demonstrated that FAPT is capable of measuring the 2D temperature distribution of an optically thin sample with sub-micron spatial resolution and sub-degree temperature resolution.

Compared to previous fluorescence-based methods, FAPT features the unique capability of transforming a regular fluorescence dye into a concentration- and excitation- independent temperature sensor, a fact that opens up the possibility of utilizing a large collection of commercially available fluorescent probes for intracellular temperature sensing applications. This advantage should facilitate the conversion of intracellular temperature mapping into a routine lab tool and make it accessible to a much broader research community. Additionally, since environmental temperature can affect cellular activities by changing enzyme activity [20], membrane characteristics [21], or ion channel gating [22], FAPT can be utilized to study the dependence of cellular thermogenesis or reaction on environmental temperature changes, a knowledge that would promote our understanding of cellular metabolism regulation and diagnosis of related diseases.

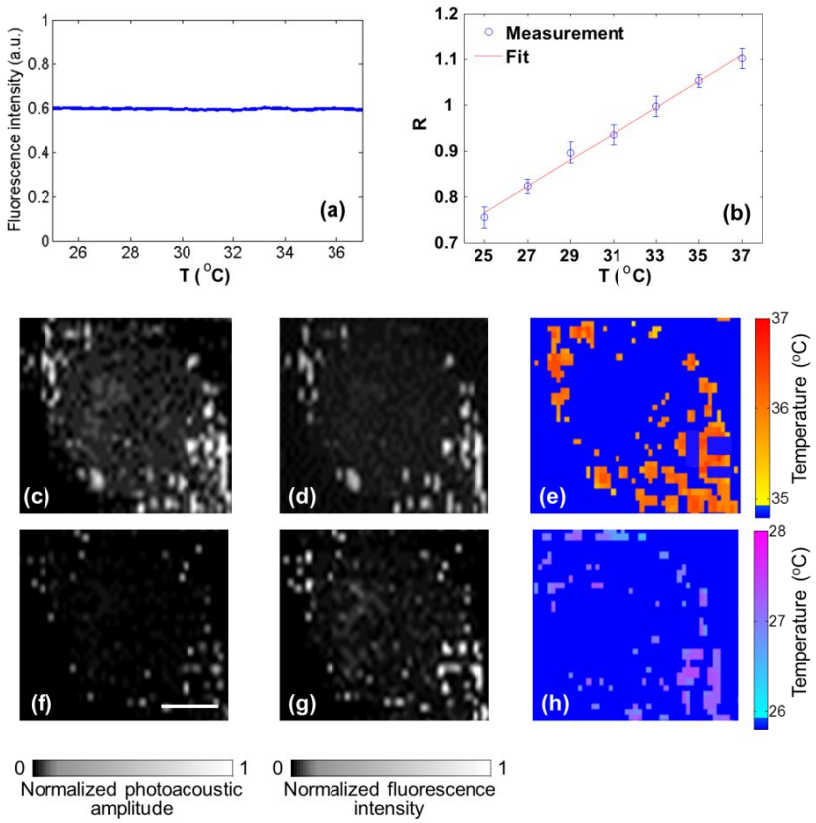

Fig. 2. Intracellular mitochondrial temperature mapping by FAPT. (a) The temperature dependence of fluorescence intensity for the fluorophore MitoTracker orange. The quantum yield of MitoTracker orange is stable over a temperature range of 25 °C – 37 °C. (b) The PA/fluorescence ratio R versus temperature for the Mito Tracker orange fluorophore. The coefficient of determination is 0.995 for the linear fit. (c)-(e) PA, fluorescence, and FAPT-recovered mitochondrial

temperature map at 36 °C. (f)-(h) PA, fluorescence, and FAPT-recovered mitochondrial temperature map at 27 °C. The dark blue background in (e) and (h) denotes unknown temperatures. Scale bar, 5 μm.

REFERENCES

1. A. Bahat, I. Tur-Kaspa, A. Gakamsky, L. C. Giojalas, H. Breitbart and M. Eisenbach, "Thermotaxis of mammalian sperm cells: A potential navigation mechanism in the female genital tract," *Nat Med* 9(2), 149-150 (2003)
2. B. B. Lowell and B. M. Spiegelman, "Towards a molecular understanding of adaptive thermogenesis," *Nature* 404(6778), 652-660 (2000)
3. Y. Kamei, M. Suzuki, K. Watanabe, K. Fujimori, T. Kawasaki, T. Deguchi, Y. Yoneda, T. Todo, S. Takagi, T. Funatsu and S. Yuba, "Infrared laser-mediated gene induction in targeted single cells in vivo," *Nat Methods* 6(1), 79-81 (2009)
4. M. Suzuki, V. Tseeb, K. Oyama and S. Ishiwata, "Microscopic detection of thermogenesis in a single HeLa cell," *Biophys J* 92(6), L46-L48 (2007)
5. C. L. Wang, R. Z. Xu, W. J. Tian, X. L. Jiang, Z. Y. Cui, M. Wang, H. M. Sun, K. Fang and N. Gu, "Determining intracellular temperature at single-cell level by a novel thermocouple method," *Cell Res* 21(10), 1517-1519 (2011)
6. F. Vetrone, R. Naccache, A. Zamarron, A. J. de la Fuente, F. Sanz-Rodriguez, L. M. Maestro, E. M. Rodriguez, D. Jaque, J. G. Sole and J. A. Capobianco, "Temperature Sensing Using Fluorescent Nanothermometers," *Acs Nano* 4(6), 3254-3258 (2010)
7. C. Gota, K. Okabe, T. Funatsu, Y. Harada and S. Uchiyama, "Hydrophilic Fluorescent Nanogel Thermometer for Intracellular Thermometry," *J Am Chem Soc* 131(8), 2766-2767 (2009)
8. L. Gao, L. Wang, C. Li, Y. Liu, H. Ke, C. Zhang and L. V. Wang, "Single-cell photoacoustic thermometry," *J Biomed Opt* 18(2), 026003-026003 (2013)
9. K. Okabe, N. Inada, C. Gota, Y. Harada, T. Funatsu and S. Uchiyama, "Intracellular temperature mapping with a fluorescent polymeric thermometer and fluorescence lifetime imaging microscopy," *Nat Commun* 3(705 (2012)
10. J. S. Donner, S. A. Thompson, M. P. Kreuzer, G. Baffou and R. Quidant, "Mapping Intracellular Temperature Using Green Fluorescent Protein," *Nano Lett* 12(4), 2107-2111 (2012)
11. I. Johnson and M. T. Z. Spence, *Molecular Probes Handbook, A Guide to Fluorescent Probes and Labeling Technologies*, Invitrogen (2011).
12. J. R. Lakowicz, *Principles of fluorescence spectroscopy*, Springer, New York (2006).
13. Y. Wang and L. V. Wang, "Förster resonance energy transfer photoacoustic microscopy," *J Biomed Opt* 17(8), 086007-086007 (2012)
14. V. L. Wang and L. Gao, "Photoacoustic microscopy and computed tomography: from bench to bedside " *Annu Rev Biomed Eng* (2014)
15. I. V. Larina, K. V. Larin and R. O. Esenaliev, "Real-time optoacoustic monitoring of temperature in tissues," *J Phys D Appl Phys* 38(15), 2633-2639 (2005)
16. P. V. Chitnis, J. Mamou, J. McLaughlan, T. Murray and R. A. Roy, "Photoacoustic thermometry for therapeutic hyperthermia," in *Ultrasonics Symposium (IUS), 2009 IEEE International*, pp. 1757-1760 (2009).
17. J. Shah, S. Park, S. Aglyamov, T. Larson, L. Ma, K. Sokolov, K. Johnston, T. Milner and S. Y. Emelianov, "Photoacoustic imaging and temperature measurement for photothermal cancer therapy," *J Biomed Opt* 13(3), (2008)
18. S. Telenkov and A. Mandelis, "Signal-to-noise analysis of biomedical photoacoustic measurements in time and frequency domains," *Rev Sci Instrum* 81(12), 124901-124907 (2010)
19. C. Zhang, K. Maslov and L. H. V. Wang, "Subwavelength-resolution label-free photoacoustic microscopy of optical absorption in vivo," *Optics Letters* 35(19), 3195-3197 (2010)
20. M. E. Peterson, R. M. Daniel, M. J. Danson and R. Eisenthal, "The dependence of enzyme activity on temperature: determination and validation of parameters," *Biochem J* 402(331-337 (2007)
21. L. Beney and P. Gervais, "Influence of the fluidity of the membrane on the response of microorganisms to environmental stresses," *Appl Microbiol Biot* 57(1-2), 34-42 (2001)
22. P. Cesare, A. Moriondo, V. Vellani and P. A. McNaughton, "Ion channels gated by heat," *P Natl Acad Sci USA* 96(14), 7658-7663 (1999)